Electronic Supporting Information

Large scale production of biocompatible magnetite nanocrystals with high saturation magnetization values through green aqueous synthesis

Marzia Marciello*, Vincent Connord, Sabino Veintemillas-Verdaguer, Manuel Andrés Vergés, Julian Carrey, Marc Respaud, Carlos J. Serna and M. Puerto Morales

Index

Experimental

Materials

Iron (II) Sulphate ($FeSO_4$), Iron (II) Chloride ($FeCl_2$), Potassium Nitrate (KNO_3), Sodium Hydroxide (NaOH), *3*-amino-propyltriethoxysilane (APTS), tetraethyl orthosilicate 98% (TEOS), carboxy methyl dextran sodium salt (CM, MW:12KDa), N-hydroxysuxccinimide (NHS), N-(3-Dimethylaminopropyl)-N'-methyl-carbodiimide hydrochloride (EDC), Ammonium hydroxide solution 25% (NH_4OH) and Phosphate Phosphate Buffered Saline solution (PBS) 10X (100 mM Phosphate and 1.54 M NaCl) were purchased by Sigma Aldrich. All the other reagents and solvents were obtained from Sigma-Aldrich.

Methods

***In vitro* magnetic fluid hyperthermia.** Complete experimental data consisting in temperature and hysteresis loop measurements as a function of magnetic field amplitude were performed on sample APTS-coated A22 MNCs (A22-A) and are shown in **Figure S10**. Integration of hysteresis loops permits to deduce a SAR value; this is shown in

Figure S10 (b) and is in very good agreement with temperature measurements. Best fit of SAR ($\mu_0 H_{max}$) curves by a power law led to $SAR \propto (\mu_0 H_{max})^{1.94}$; the corresponding curve is shown in **Figure S10** (b). The rather closed hysteresis loop and the power exponent close to 2 are two indications that these MNPs are closer to the superparamagnetic regime than the ferromagnetic one.[1] Hysteresis loop curves show that these coated MNCs are almost saturated in a 44 mT and display a rather large magnetization, even at high-frequency. This confirms both their structural quality and indicates that they have a low anisotropy, which is a very good point for their hyperthermia properties, even in the presence of magnetic interactions.[2]

MNCs surface modification.

A22-A. MNCs have been directly coated with APTS using four different MNCs/ APTS ratios (w/w), 1:4, 1:10, 1:30 and 1:100. Hydrodynamic size and isoelectric point were measured (**Figure S11**). Hydrodynamic size of APTS coated MNCs was reduced respect to uncoated MNCs for all ratios except for the relation MNCs/APTS 1:100 (w/w). Smallest size was obtained with 1:4 ratio (w/w). The isoelectric point was not significantly changed respect to the uncoated nanocrystals and no difference between the four APTS coated MNCs was observed to indicate a poor functionalization probably due to a low amount of hydroxy groups on MNCs surface (**Figure S11**).

A22-T. To coat MNCs with TEOS, different ratios MNCs/TEOS (w/w) were investigated (1:1, 1:1/2, 1:/3, 1:1/4, 1:1/5, 1:1/7) (as reported in Experimental in main text), for the lowest amounts of TEOS the experimental time was increased to 30 minutes. Smaller hydrodynamic size values were obtained using a relation TEOS/MNCs 1:1 and 2:1 (w/w). With the others amounts of TEOS the hydrodynamic size was

increased respect to the uncoated MNCs (**Figure S3**). A22-T MNCs prepared by TEOS/MNCs ratio 1:1 and 2:1 showed a significant isoelectric point shift to lower pH values (pH 2.5 and 3.8 respectively) (**Figure S3**).

A22-TA. MNCs coated with TEOS in a ratio A22/TEOS 1:1 was chosen to be coated with APTS. Different amounts of APTS were studied (1:4, 1:10, 1:50, 1:100 (w/w)).
The smallest hydrodynamic size was obtained with a ratio A22-T/APTS 1:50 (w/w) (**Figure S4**). Isoelectric value was moved from 2.5 to 7 with the MNCs/APTS ratios 1:50 and 1:100 (w/w). Smaller amounts of APTS showed only a small isoelectric point shift to lower pH (**Figure S4**).

Preliminary studies of A22-TAD stability in PBS buffer

At 1 ml of a suspension containing A22-TAD at 60 μg Fe/ml 100 μl of PBS buffer 10 X were added. Hydrodynamic sizes of the coated nanoparticles in PBS as a function of the time were measured (0, 0.5, 4, 24, 48 h). A small aggregation of A22-TAD was observed at the different times. After 24 h the aggregation was kept constant (~ 450 nm) (**Table S1**).
This aggregation is probably due to a loss of the colloidal stability for dextran negatively charges due to the presence of other ions in the suspension. Furthermore nanocrystals precipitation is helped by their large size and their high magnetic moment which guarantee strong magnetic interactions. More experiments studying the influence of magnetic nanocrystals concentration on MNCs aggregation in PBS buffer pH 7.4 are in progress. Although the dextran coating is not sufficient to achieve colloidal stability of these large iron oxide nanoparticles at pH 7 in high salinity buffers, this is the first

step to further functionalize the MNCs with biomolecules to transform them into multifunctional platforms.

References

1 J. Carrey, B. Mehdaoui and M. Respaud, *J. Appl. Phys.*, 2011, **109**, 083921.

2 B. Mehdaoui, R. P. Tan, A. Meffre, J. Carrey, S. Lachaize, B. Chaudret and M. Respaud, *Phys. Rev. B*, in press, arXiv:1301.5590.

Supplementary Figures

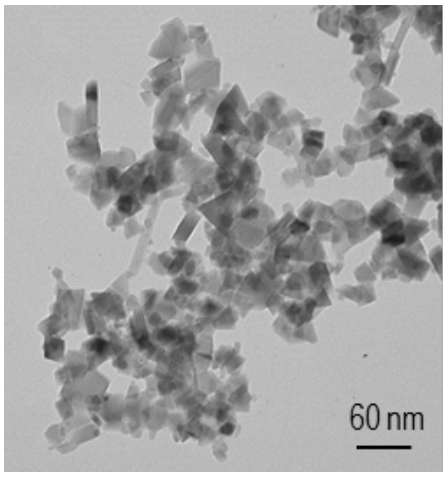

Figure S1. TEM micrograph of MNCs synthetized in the presence of air.

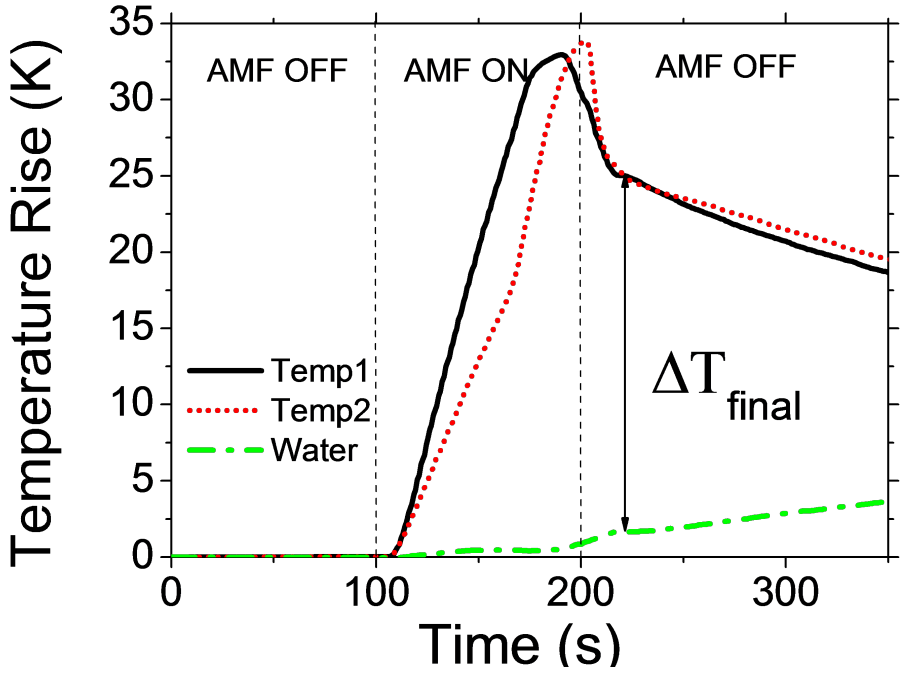

Figure S2. Typical example of a temperature rise curve during the AFM application (100s, noted AMF ON). Measurements on A22 at 44mT/70kHz is shown. "Temp1" and "Temp2" are probes introduced at the bottom and the top of a calorimeter; "Water" is a probe introduced in the blank sample. After the magnetic field is switched off, the sample is shaken for temperature homogenization. The temperature rise ΔT_{final} used for SAR calculation is shown as a double-ended arrow.

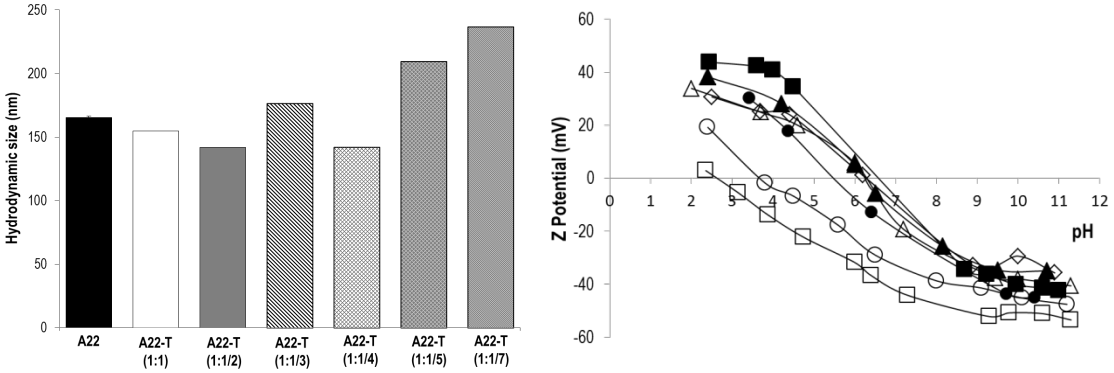

Figure S3. Left: Hydrodynamic size of TEOS coated MNCs (A22-T) prepared in different A22/TEOS (w/w); Right: Isoelectric point of TEOS coated MNCs with different ratios MNCs/TEOS (w/w) (■ A22, □ A22-T (1:1), ○ A22-T (1:1/2), ● A22-T (1:1/3), ▲ A22-T (1:1/4), Δ A22-T (1:1/5), ◊ A22-T (1:1/7)) in comparison with uncoated MNCs.

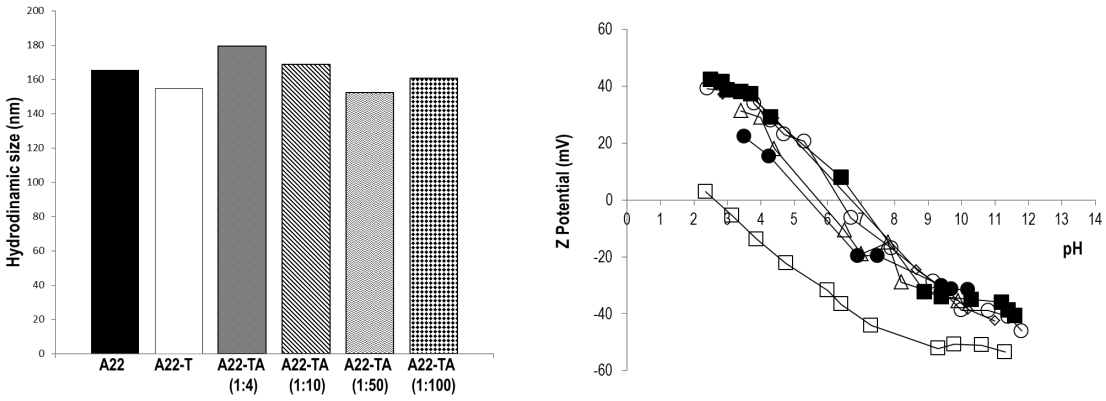

Figure S4. Left: Hydrodynamic size of A22-TA prepared in different A22-T/APTS ratios (w/w) compared with A22-T and A22 MNCs; Right: Isoelectric point of APTS-TEOS coated MNCs with different ratios A22-T/APTS (w/w) (■ A22, □ A22-T, ● A22-TA (1:4), Δ A22-TA (1:10), ◊ A22-TA (1:50), ○A22-T (1:100)) in comparison with uncoated MNCs.

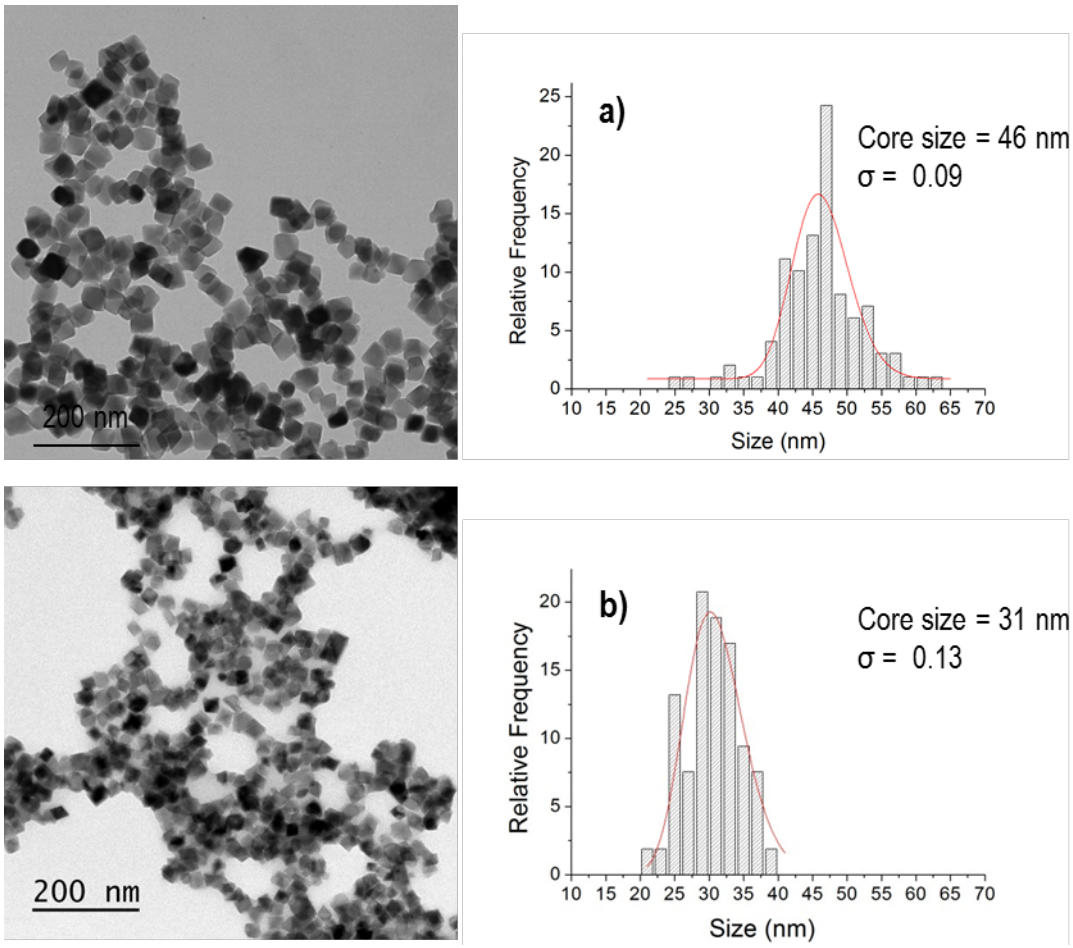

Figure S5. TEM micrographs and size distribution (adjusted to Log-normal functions) of nanocrystals synthetized with the same chloride iron (II) salt (0.025M) and NaOH (0.07M) concentration: a) only in the presence of water; b) in the presence of water/ethanol 50:50 (v/v).

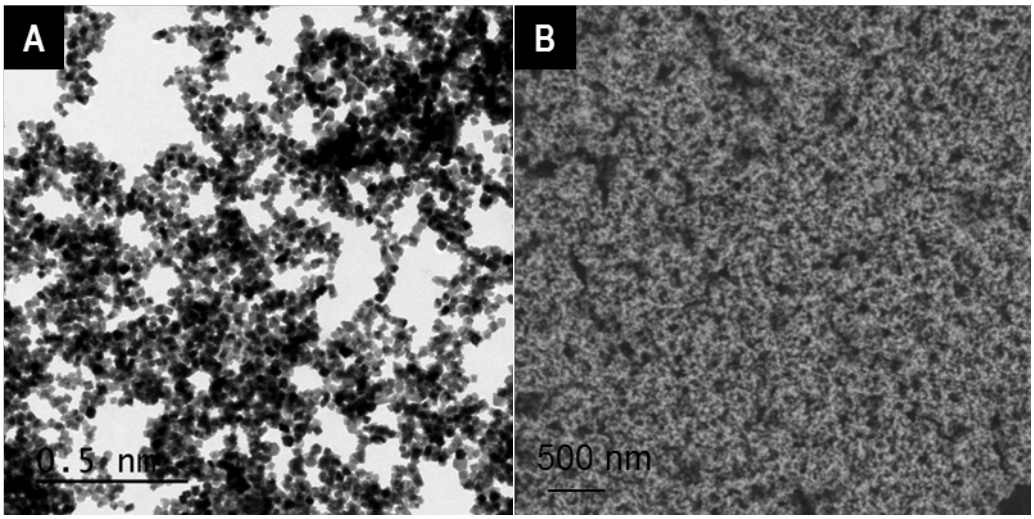

Figure S6. TEM (A) and SEM (B) micrographs of scale-up A22 synthesis.

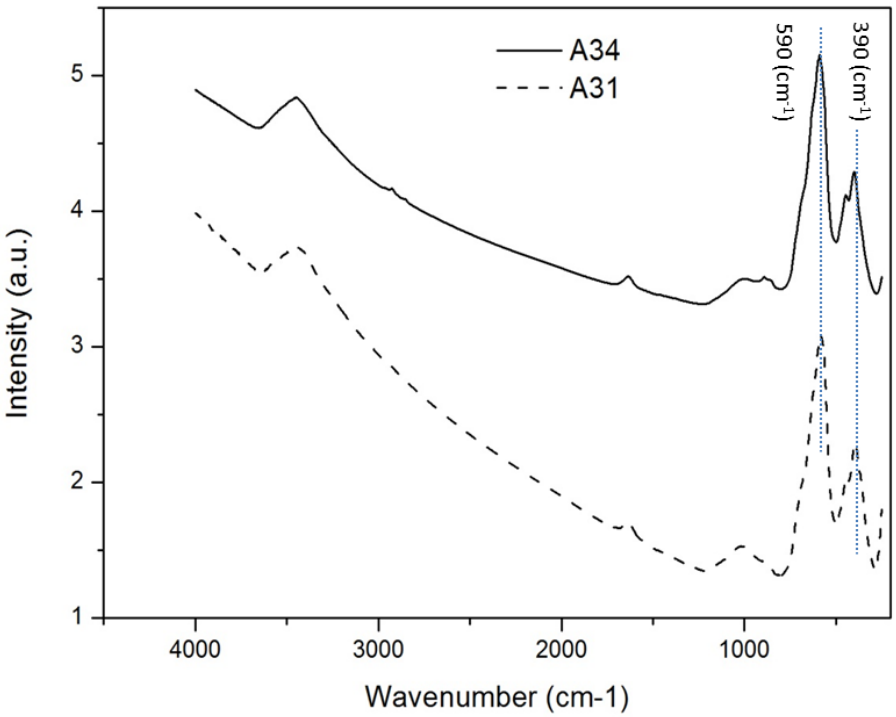

Figure S7. FT-IR spectra of magnetite nanocrystals synthesized from different iron salts (A34 from $FeSO_4$ and A31 from $FeCl_2$).

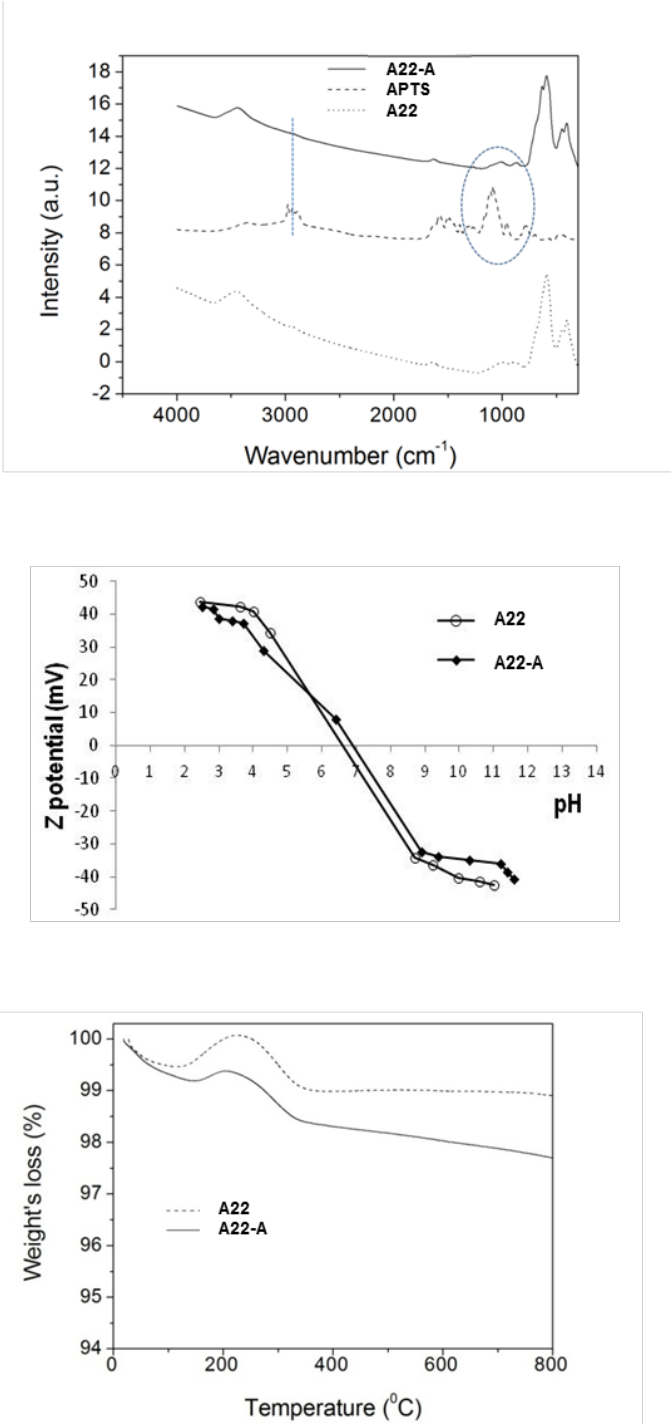

Figure S8. Top: FT-IR spectra of MNCs coated directly with APTS (A22-A) compared with the uncoated ones (A22) and APTS; Medium: Z potential values of MNCs directly coated with APTS (A22-A) compared with the uncoated ones; Bottom: TG curves of MNCs directly coated with APTS compared with the uncoated ones.

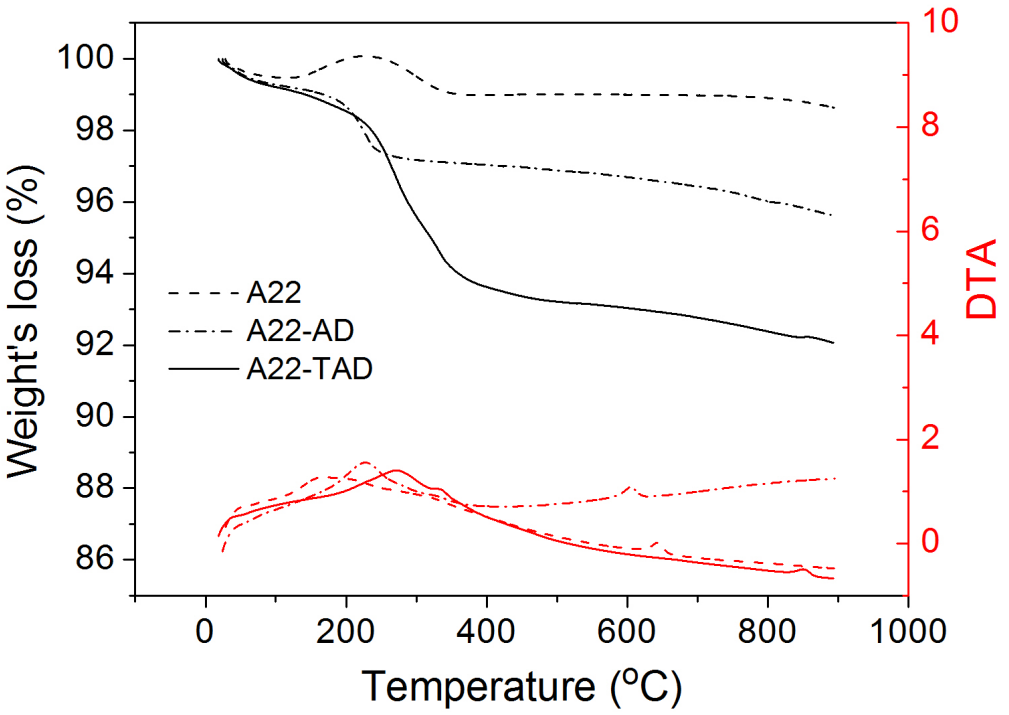

Figure S9. TG and DTA curves of D coated A22-TA and A22-A (A22-AD) MNCs compared with the uncoated ones.

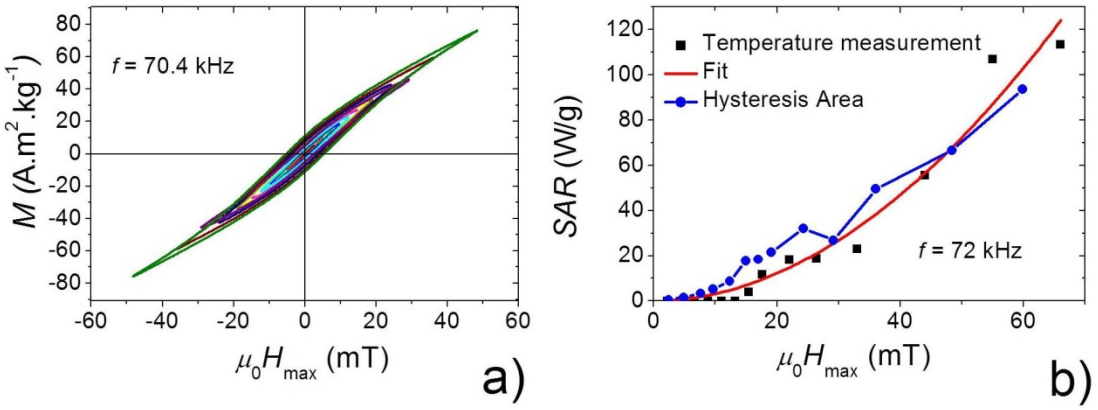

Figure S10. Heating properties of sample A22-A as a function of magnetic field. a) Hysteresis loop measurements at f = 70.4 kHz; b) SAR as a function of magnetic field: comparison between the temperature measurements (square dots), the corresponding best fit (line) and the SAR calculated from the hysteresis area (round dots).

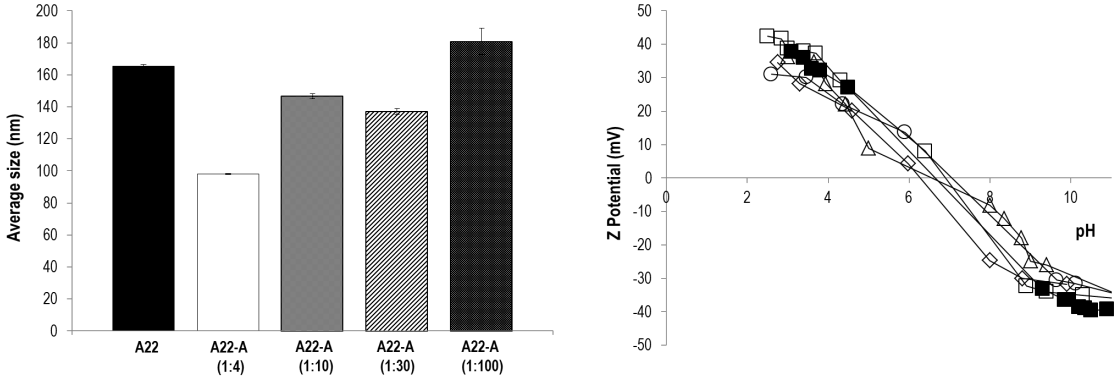

Figure S11. Left: Hydrodynamic size of APTS coated MNCs with different ratios MNCs/APTS (w/w) in comparison with the uncoated ones; Right: Isoelectric point of APTS coated MNCs with different ratios MNCs/APTS (w/w) (■ A22, □ A22-A (1:4), Δ A22-A (1:10), ○ A22-A (1:30), ◊ A22-A (1:100)) in comparison with uncoated MNCs.

Table S1. Hydrodynamic size and polydispersion index values of A22-TAD in the presence of PBS buffer pH 7.4 *vs* time.

Time (h)	Hydrodynamic size (nm)	Polydispersion Index
0	130	0.19
0.5	237	0.35
4	380	0.26
24	450	0.27
48	504	0.26